
FINITE ELEMENT ANALYSIS OF THE SEISMIC BEHAVIOR OF THE ASSEMBLED LIGHT STEEL FRAME- LIGHT WALL STRUCTURES

Liu Wenchao^{1,2}, Chen Zheng³, Wang Cheng¹, Dong Hongying³, Wang Ruwei³*

- 1. Technology Research and Development Center, CCCC Fourth Highway Engineering CO.,LTD., Beijing 100022, China; liuwenchaoann@foxmail.com*
- 2. Office of Postdoctoral Research, Beijing University of Technology, Beijing 100124, China; liuwenchao@bjut.edu.cn*
- 3. Key Laboratory of Urban Security and Disaster Engineering, Beijing University of Technology, Beijing 100124, China; chenzhengbjut@foxmail.com*

ABSTRACT

In order to meet the needs of the development of low-rise assembly structure in rural areas, a fabricated light-weight steel frame-composite light wall structure is proposed in this paper. The light-weight steel frames are used to bear the vertical loads. The single-row-reinforced recycled concrete wall-boards are used as lateral members to resist most of the horizontal earthquake loads. The wall-board, EPS (Expanded Polystyrene) insulation modules, and fly ash blocks form the thermally insulated wall. Four fabricated lightweight steel frame-composite light wall structures and one light-weight steel frame (FRA) structure were tested under the low cyclic loads. The influence of wall reinforcement spacing and structural form (be it fly ash block or not) on the seismic performance of this new structure was analysed and the damage process of the specimen was simulated using the ABAQUS[®] software. The results show that the light steel frames and the single-row-reinforced recycled concrete wall-board can work well together. Furthermore, the structure has two clear seismic lines. Due to the use of EPS insulation modules and fly ash blocks, the structure has good anti-seismic and thermal insulation abilities. Reducing the spacing of bars or compositing fly ash blocks can significantly improve the seismic performance of the structure. The finite element method (FEM) calculations agreed well with the experimental results, which validates the proposed model.

KEYWORDS

Pre-fabricated construction, Rural residence, Fabricated light-weight steel frame- composite light wall structure, Seismic performance, Experimental study

INTRODUCTION

Due to rapid growth in the sector of construction and low production costs, pre-fabricated construction has attracted the attention of many scholars in the early 20th century. By the 1960s, pre-fabricated construction had preliminarily been established in developed countries, such as Great Britain, France and the former Soviet Union. China began to vigorously develop pre-fabricated construction in 2015, and introduced a series of related measures. In November 2015, the Ministry of Housing and Urban-rural Development issued the "Outline for the modernization and development of the construction industry", and in February 2016, the state council issued the "Guidelines on the vigorous development of prefabricated construction", both of which clearly pointed out the development of pre-fabricated construction. According to some statistics, at present, the construction of villages and towns accounts for more than 50% of the total buildings in China. There is only a handful of research on the structural technology suitable for pre-fabricated construction in villages and towns. Villages and towns are in urgent need of developing new assembly-type structural systems.

Domestic and foreign scholars have conducted a lot of research on the assembled residential systems. Serrette et al. studied the thin-walled light steel structure, and carried out a series of tests and theoretical analyses on the lateral resistance of light steel keel composite wall [1-4]. Based on the frame of the concrete light wall structure, Tsinghua University developed SW structure [5]. Hao et al. (2010) developed the CL building system based on the welded steel grid technology [6]. Beijing University of Civil Engineering and Architecture developed the LI+T composite concrete building system (2007), in which the connection between different types of wall-boards is unified, whereas the number of structural nodes is also reduced [7]. Xi'an University of Architecture and Technology and Beijing Jiaotong University jointly developed the energy saving system having multi-ribbed composite plate and light frame structure (2010), which is suitable for high-rise earthquake-resistant structures consisting of pre-fabricated components and integral pouring of external frames [8].

Mochizuki tested the seismic performance of vertical joints of pre-cast concrete shear wall, and found that the ultimate bearing capacity of the wall was related to the constraint conditions of horizontal joints (including pin action). Chen et al. (2012) carried out low-cycle repeated load test on the one-half reduced scale four-storey space model of the full-prefabricated shear wall structure, and showed that the yield load is much higher than the seismic shear force, whereas the test piece maintained elasticity under medium earthquake and therefore, can meet the fortification target of large earthquakes [10]. Cao et al. (2017) carried out an experimental study on the seismic performance of semi-assembled low-rise recycled concrete shear wall, and the results showed that, under horizontal load, horizontal crack and a small slip appear in the joint connection between the pre-cast shear wall and the foundation wall, whereas the structure had good seismic performance [11].

Many studies have been conducted on the seismic performance and connection performance of light steel shear wall. Most of them have focused on industrial and high-rise

buildings. However, research on the seismic performance of pre-fabricated light steel frame-composite light wall structure, suitable for rural residential buildings, has not been reported in literature. To this end, the low-cycle cyclic load tests of four assembled light-weight steel-light wall structure and one light-steel hollow frame were designed. This paper studies the influence of construction measures (be it the composite fly ash block layer or not) and spacing of distributed bars on the bearing capacity, hysteretic characteristics, ductility, stiffness and failure mode of the wall structure, and provides a reference for the design of assembled structure of rural buildings.

EXPERIMENTAL

Material Properties

The specimen was made of 42.5 grade ordinary Portland cement, in which the replacement of recycled coarse aggregate(RCA) was 100% (particle size of 5-10 mm). The recycled coarse aggregate was made up of crushed concrete of a demolished building in Beijing, China. Fine aggregate used natural sand (aggregate size 0-5 mm). All aggregates were mixed with tap water. The mixing ratio and cubic compressive strength (f_{cu}) of recycled aggregate concrete is presented in Table 1.

The measured concrete strength is presented in Table 1. The mechanical properties of the steel used in the test piece are given in Table 2. The EPS modules were used as the insulation layer. The compressive strength of fly ash blocks, used in the specimen, was 2.35 MPa. The M10 mixed mortar (The strength representative value is 11.5MPa~16.0MPa) was used for building the specimen.

Tab. 1 - Mixing proportion and cubic compressive strength of the specimen (kg/m^3)

RCA/%	Cement	Fly ash	Mineral powder	Sand	Recycled pebble	Water reducer	Water	f_{cu}/MPa
100	369	78	78	841	841	3.5	181	43.6

Tab. 2 - Mechanical properties of steel bar and steel tube

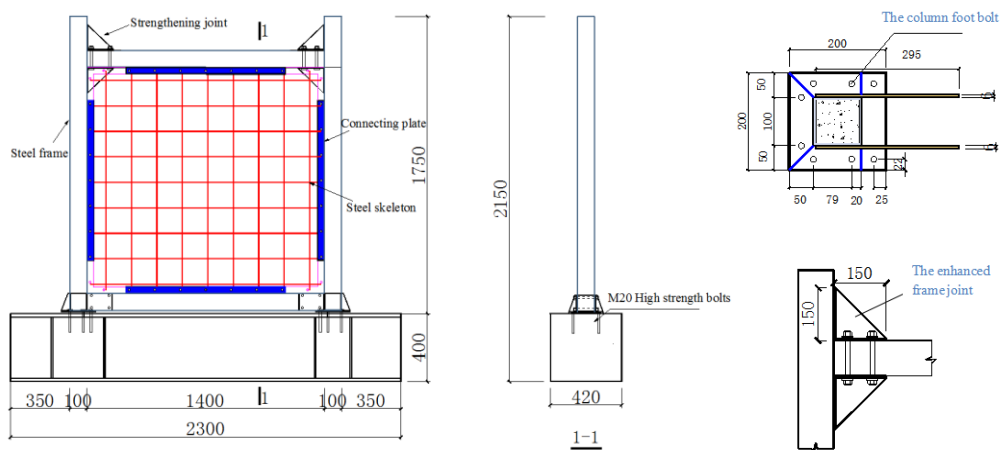
Steel type	Steel size /mm	Yield strength f_y /MPa	Ultimate strength f_u /MPa	Elongation δ %	Modulus of elasticity E /MPa	Thickness /mm
Steel bar	D5	680	786	5.5	2.09×10^5	—
Steel plate	—	309	467	25.27	2.11×10^5	4
Steel tube	100×100	375	477	23.23	2.18×10^5	4

Details of the Test Specimens

Four fabricated light-weight steel frame-composite light wall structures and one light-weight steel frame structure were designed. The main parameters of the specimens are presented in Table 3. The light-weight steel frames were constructed of square steel tubes having the thickness of 4 mm and which were filled with recycled concrete. In order to facilitate the bolt connection with the single-row-reinforced recycled concrete wall-boards, steel plate with the thickness of 4 mm was welded. The frame joint was enhanced, and the column foot was provided with 8 bolt holes to facilitate the connection with the I-foundation. The column foot bolt adopted M20 high-strength bolt. The recycled concrete wallboard was composed of frame steel plate with the thickness of 4 mm and distributed reinforcement with a diameter of 5 mm. The connecting bolt of the wall-board was M10. The single-row distributed reinforcement of wall-board was placed in two directions. The reinforcement ratio of the distributed rebar was 0.33%~0.49%. The size and reinforcement details of the specimens are shown in Figure 1.

Tab. 3 - Main parameters of the specimens

Serial No.	Wallboard thickness/mm	Reinforcement spacing/mm	EPS module thickness /mm	Fly ash block thickness /mm
PFS40-S1-1	40	100	70	-
PFS40-S1-2	40	100	70	60
PFS40-S2-1	40	150	70	-
PFS40-S2-2	40	150	70	60
FRA	-	-	-	-



(a) Details of the specimen



(b) Construction of the specimen

Fig. 1 - Size and reinforcement details of specimens

Test Set-Up and Loading Programme

In this work, low cyclic load method was adopted for the tests. In this regard, 600 kN vertical load was applied at the top center of the distribution beam, which remained constant during the loading process. The loading field is shown in Figure 2(a). The horizontal load was applied at the center of the frame beam. The loading point was 1480 mm from the top of the foundation, and the axial compression ratio was 0.35. In order to prevent the out-of-plane instability of specimens during loading, lateral restraint braces were set in the vertical direction of horizontal loading. The column base of the specimen was fixed to the steel beam of the foundation using high-strength bolts, and the steel beam of the foundation was fixed to the ground using ground anchor bolts.

The measured horizontal displacement of the loading point was used as the control displacement. When the displacement angle was less than $1/500$, the displacement loading increment was $1/2500$. When the displacement angle was less than $1/50$, the displacement loading increment was $1/500$. When the displacement angle was greater than $1/50$, the displacement loading increment became $3/500$, which was twice per stage. During the whole testing process, the displacement loading rate was consistent. It is stipulated that the force was positive when the horizontal jack was pushed out. The magnitude of the displacement loading is shown in Figure 2(b).

Force sensors are arranged at the ends of vertical and horizontal jacks. At the loading height, the horizontal displacement meter is arranged at the end of the loading beam.

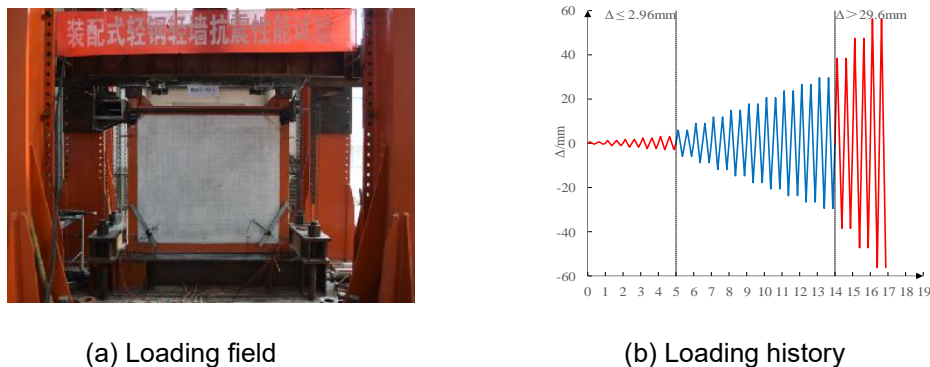


Fig. 2 - Loading device and the loading history

RESULTS AND DISCUSSION

Failure Characteristics

The obvious shear failure took place in the wall, which indicated that the wall undertook a lot of horizontal shear force. With the wall cracked, the light steel frame became the main force-bearing member at the later stage of loading. It finally underwent bending failure, while no obvious

damage was found in the joint. The structure had two clear seismic lines. In the later stage, the connecting members between the wall and the frame were not obviously damaged, which indicated that the two components worked well together. With the increase of reinforcement ratio, the width of diagonal crack in the wall obviously decreased. The damage of the wall with fly ash layer was not obvious, which indicated that fly ash block could effectively withstand the horizontal force of the wall. Figures 3(a) - 3(h) show the ultimate failure models and crack distribution of specimens.

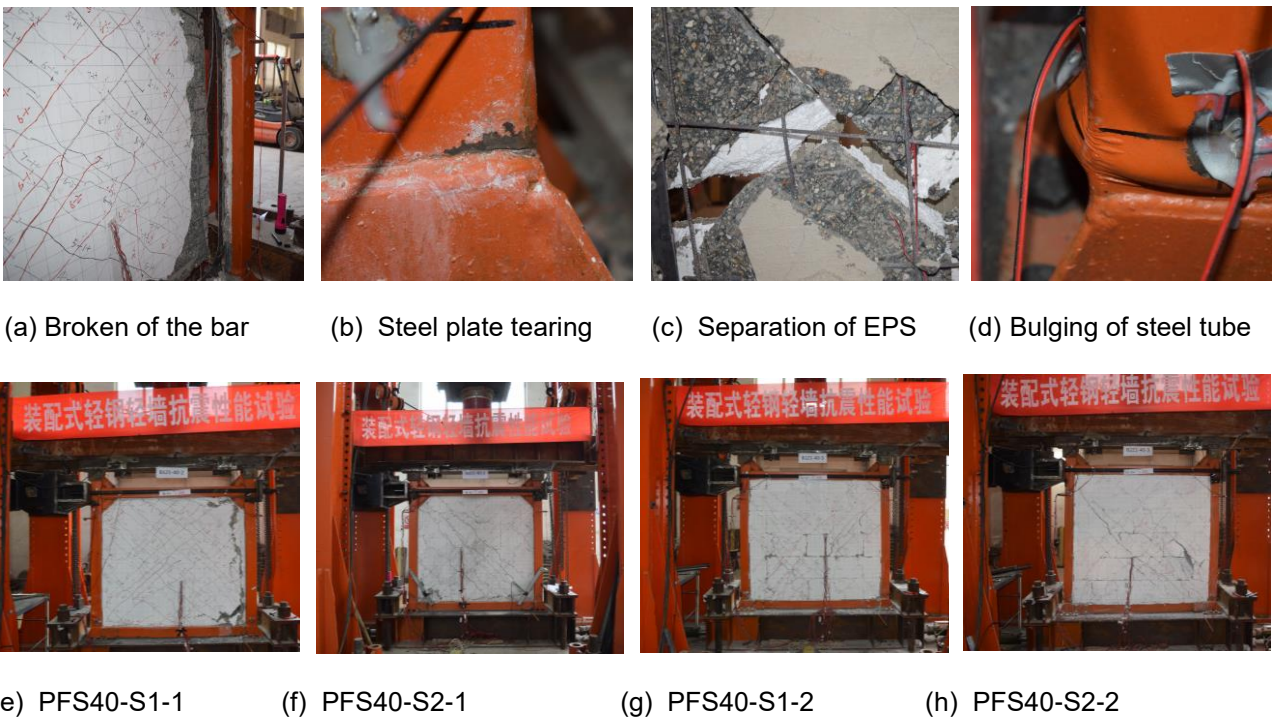


Fig. 3 - Failure models and crack distribution of specimens

Load-Displacement Response

The measured characteristic results of specimens on the skeleton curve are presented in Table 4. In Table 4, F_y is the yield load, F_u is the peak load, and F_d is the failure load. Furthermore, Δ_c , Δ_y , Δ_u and Δ_d are the displacement values corresponding to F_c , F_y , F_u and F_d , respectively. Additionally, θ_c , θ_y , θ_u and θ_d are the corresponding interlayer displacement angles. The yield load is determined by energy equivalence method. The failure load is the corresponding load value when the peak load drops to 85%. The skeleton curves of specimens are shown in Figure 4.

Tab. 4 - Measured characteristic results of the specimens

Serial No.	F_y /kN	Δ_y /mm	F_u /kN	Δ_u /mm	F_d /kN	Δ_d /mm	μ
PFS40-S1-1	784.10	7.35	920.63	10.12	800.95	13.63	1.85
PFS40-S1-2	966.71	7.18	1141.11	11.44	969.95	14.88	2.07
PFS40-S2-1	623.27	7.87	731.89	11.10	622.10	13.71	1.74
PFS40-S2-2	797.68	7.20	936.34	9.82	795.89	14.85	2.06
FRA	120.74	26.83	143.56	47.54	122.03	64.89	2.42

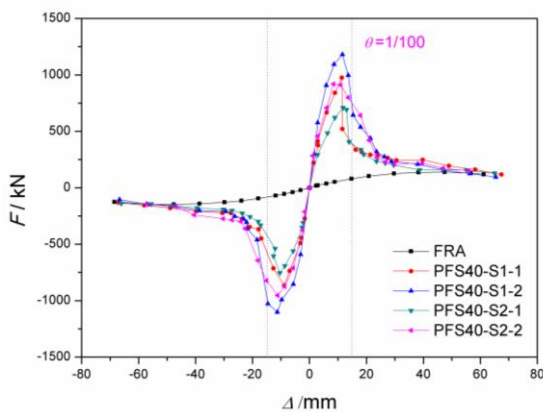


Fig. 4 - Skeleton curves of specimens

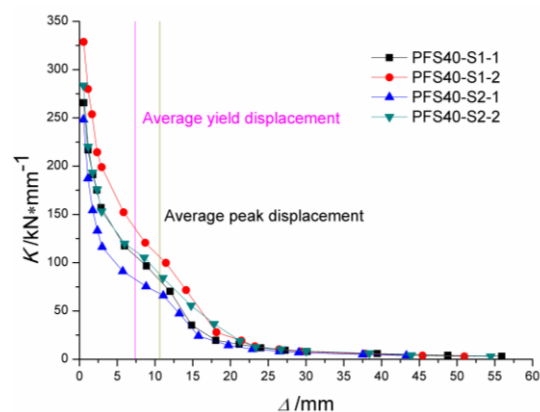


Fig. 5 - "Ki-Δ" curves of specimens

Compared with the specimens without filled fly ash block, the bearing capacity of the specimens filled with fly ash block was significantly increased. The yield loads of PFS40-S1-2 and PFS40-S2-2 increased by 18.9% and 21.9%, respectively, indicating that the bearing capacity of the structure significantly increased due to the filling by fly ash block. The wall reinforcement spacing had a relatively large impact on the bearing capacity of the structure. Compared with PFS40-S2-1 and PFS40-S2-2, the peak loads of PFS40-S1-1 and PFS40-S1-2 increased by 20.5% and 17.9%, respectively. The ultimate bearing capacity of light-weight steel frame was 139.61 kN. The ultimate bearing capacity of light-weight steel frame-composite light wall structures was 424.24% - 825.33% higher than that of light-weight steel frame.

The proposed structure meets the requirements of the Chinese Code for seismic design of buildings [12], which states that the elastic-plastic displacement angle of steel structure is limited to 1/50 and the failure displacement angle of specimen FRA is 1/23. The results show that the recycled concrete light-weight steel frame has good collapse resistance. Meanwhile, the elastic-plastic ultimate displacement angle of specimens PFS-S1-2 and PFS-S2-2 with fly ash filled layer meet the requirement, which states that the elastic-plastic displacement angle of reinforced concrete frame - seismic wall should not be higher than 1/100.

It is assumed that the weight of low-rise buildings is about 1.5T per square meter. For a 150 m² house, the total mass is about 225t. In the case of 8 degree seismic fortification intensity, the maximum value of the basic seismic acceleration is 0.3g, whereas the horizontal load is calculated

to be 675 kN. Furthermore, the average yield load of the wall specimen is 792.94 kN, while the overall structure is controlled within the elastic working range.

$$\mu = \frac{|\Delta_d| + |-\Delta_d|}{|\Delta_y| + |-\Delta_y|} \quad (1)$$

The displacement ductility coefficient μ is the ratio of Δ_d (failure displacement) to Δ_y (yield displacement). Since the hysteresis curve is not completely symmetrical, the displacement ductility coefficient is calculated according to Equation (1).

- 1) The recycled concrete light steel frame has good ductility, whereas the maximum failure displacement can reach the value of 64.89 mm. Compared with the light-weight steel frame, the ductility of the structure is reduced after the wall-board is assembled.
- 2) The specimens PFS40-S1-2 and PFS40-S2-2 filled with fly ash block have larger peak and failure displacements. Meanwhile, the ductility coefficient is also higher, which indicates that fly ash block can effectively improve the ductility of the structure.
- 3) Reducing the spacing of distributed reinforcement or increasing the reinforcement ratio of distributed reinforcement can effectively improve the ductility coefficient of the structure.

Stiffness and Degradation

The stiffness-displacement K_i - Δ curves of specimens as shown in Figure 5. In this study, K is the secant stiffness of peak points at different time intervals. As shown by the results presented in Table 5, K_0 , K_y , K_u and K_d represent the average values of secant stiffness of hysteresis curve in the initial stage, yield load, peak load and failure load, respectively. The K_i - Δ curves of specimens are obtained using Equation (2).

$$K_i = \frac{|+F_i| + |-F_i|}{|\Delta_i| + |-\Delta_i|} \quad (2)$$

where i is the number of cycles, K_i is the tangential stiffness of the i -th cycle, F_i is the peak load corresponding to the i -th cycle, and +, - represent the positive and negative directions of the horizontal force.

Tab. 5 - Experimental results of stiffness and degeneration coefficient

Serial No.	K_0 /(kN·mm ⁻¹)	K_y /(kN·mm ⁻¹)	θ_y	K_u /(kN·mm ⁻¹)	θ_u	K_d /(kN·mm ⁻¹)	θ_d
PFS40-S1-1	265.48	106.68	1/201	90.97	1/146	58.76	1/108
PFS40-S1-2	304.88	134.73	1/206	99.75	1/129	65.18	1/99
PFS40-S2-1	248.24	79.20	1/188	65.97	1/133	45.38	1/107
PFS40-S2-2	283.41	110.87	1/206	95.35	1/151	53.60	1/100
FRA	15.88	4.50	1/55	3.02	1/31	1.88	1/23

The degradation of stiffness of light-weight steel frame-composite light wall structure can be divided into five stages, namely the Initial stage, the cracking stage, the yield stage, the limit stage, and the failure stage. The specimens have the character of higher initial stiffness, while the stiffness decreases rapidly with the cracking of the wall. When the wall is seriously damaged, the frame beam and the column are severely deformed. Then, the stiffness of the test piece continues to decrease, though the rate of decrease drops down significantly.

In the case of same reinforcement spacing, the structure with fly ash block layer had higher yielding stiffness, peak stiffness and failure stiffness. Compared with PFS40-S1-1 and PFS40-S2-1, the average initial lateral stiffness of PFS40-S1-2 and PFS40-S2-2 increased by 12.92% and 12.41%, respectively. In addition, the average yield stiffness increased by 20.82% and 28.56%, and the average peak stiffness increased by 8.75% and 30.81%, respectively. Fly ash block significantly delayed the structural damage during the process of loading.

In the case of same structural form, the spacing of distributed reinforcement bars has a great influence on the characteristic stiffness of the specimen. Smaller the spacing of reinforcement bars, higher was the characteristic stiffness of the specimen. The initial stiffness of the light steel frame structure was 15.88 kN·mm⁻¹. Compared with the light-weight steel frame structure, the initial stiffness of the new structure increases by 1463.22 - 2002.20.

Energy Dissipation Capacity

The area of intersection of characteristic point load skeleton curve and coordinate axis is taken as the energy dissipation value. Furthermore, E_y is the yield energy dissipation, E_u is the peak energy dissipation and E_d is the destruction energy dissipation. Additionally, E_p is the cumulative total energy consumption, which is the cumulative area of the cyclic hysteresis loop when the specimen is destroyed. The experimental results of energy dissipation are presented in Table 6.

Tab. 6 - Experimental results of the energy dissipation

Serial No.	E_y	E_u	E_d	E_p
PFS40-S1-1	7.651	11.383	13.08566	153.465
PFS40-S1-2	9.586	17.261	20.855.92	214.786
PFS40-S2-1	6.912	10.101	12.85783	138.214
PFS40-S2-2	8.714	14.858	19.45049	198.689
FRA	4.510	9.388	13.12238	23.584

Compared with the light steel frame FRA, E_y , E_u and E_p increased by 112.55%, 58.93%, and 810.7%, respectively, indicating that the energy-dissipation capacity of the assembled wall-board can be significantly improved.

Compared with PFS40-S1-1 and PFS40-S2-1, the energy consumption of specimens PFS40-S1-2 and PFS40-S2-2 increased by 59.4% and 51.3%, indicating that the energy consumption of the structure can be significantly improved by filling fly ash blocks. Under the same structural form, the wall reinforcement spacing has little effect on the energy dissipation capacity of the specimens. As shown in Figure 6, comparing with PFS40-S2-1 and PFS40-S2-2, the damage energy consumption of PFS40-S1-1 and PFS40-S1-2 increased by only 2% and 7%, respectively.

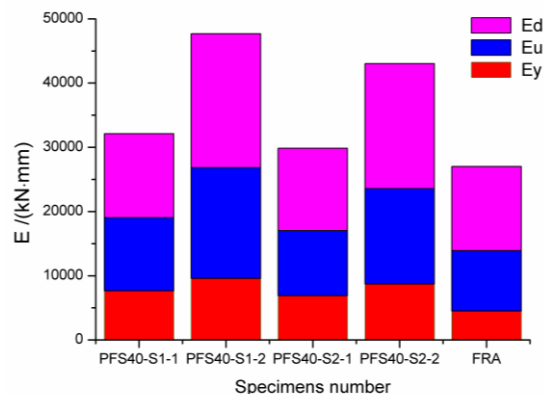


Fig. 6 - Energy dissipation histogram of specimens

FEM ANALYSIS

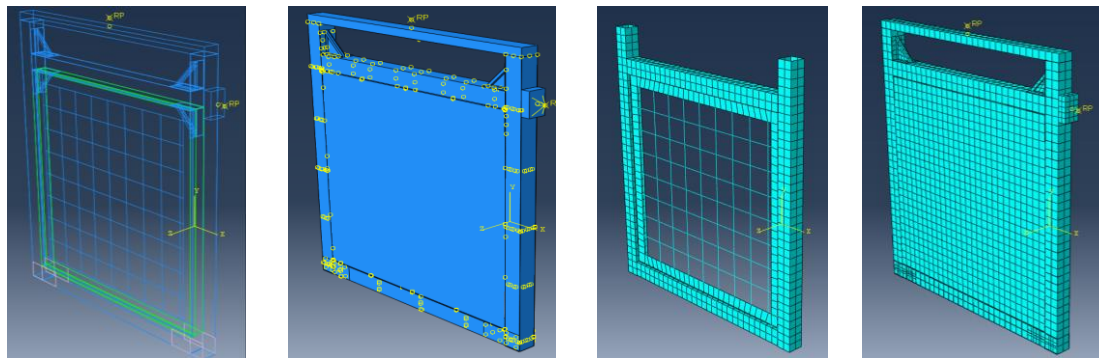
Finite Element Parameters

The damage-plasticity model of concrete is adopted in the calculations. The constitutive relation of the concrete in square steel tube is restrained by square steel tube as proposed by Cai [13], which is based on Mander [14] model. The compressive constitutive relationship of fly ash

block wall was adopted, as proposed by Wang [15]. The constitutive relation of steel adopted the double broken line model. The contribution of EPS module to shear capacity was ignored.

Finite Element Model

The solid element C3D8R was used to simulate the steel tube, concrete and fly ash. The truss element T3D2 was adopted for reinforcement of the wall-board, while the shell element S4R was adopted for the steel plate of the wall-board. The steel bars are modelled separately without considering the bond slip between the steel bars and the concrete. The model is divided using hexahedral structured mesh, and the shell element is divided using the tetrahedron-main unit free mesh, as shown in Figure 7.



(a) Constructional detail (b) Boundary condition (c) Steel skeleton (d) Wall structure

Fig.7 - Calculation models and meshing

Analysis of the Calculated Results - The Skeleton Curve

The comparison between the calculated and measured curves of force-displacement $F-\Delta$ is shown in Figure 8.

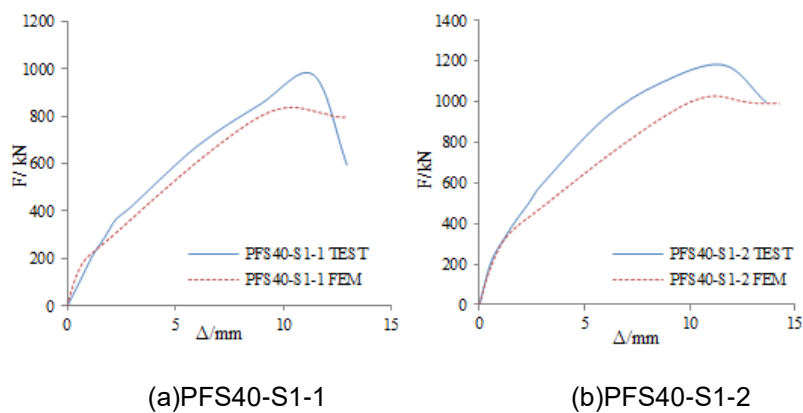


Fig. 8 - Comparison between the calculated and measured curves of $F-\Delta$

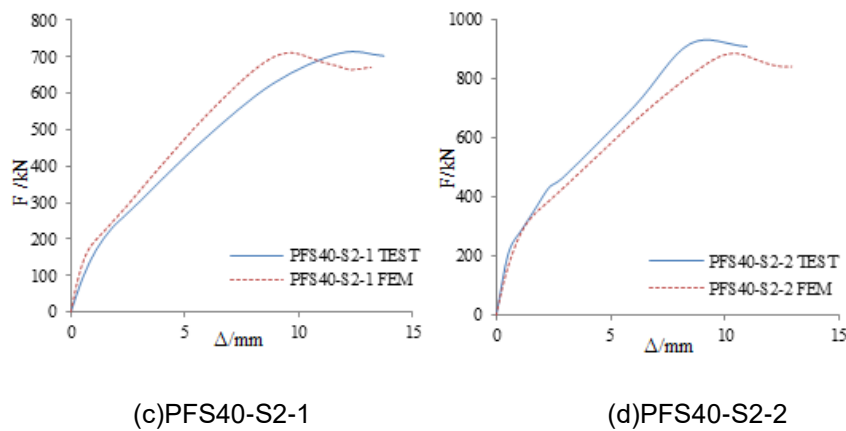


Fig. 8 - Comparison between the calculated and measured curves of $F-\Delta$

Figure 8 shows that, at the early stage of load, the calculated curve is in good agreement with the measured curve. While in the middle and late stages, the calculated results lie below the measured ones, whereas the error between the calculated and measured values of ultimate load is less than 15%.

CONCLUSIONS

- (1) The fabricated lightweight steel frame-composite light wall structure has two anti-seismic lines of composite light wall and light steel frame. The structure has good seismic performance. The EPS module and the fly ash filling layer can effectively slow down the structural damage process.
- (2) The structural form has a significant impact on the seismic performance of the structure. Filling the fly ash block can effectively improve the seismic performance of the structure. The spacing of reinforcing bars has a relatively small impact on the energy consumption performance. It is suggested that the reinforcement ratio of reinforcing bars, distributed on the wall-board, should be controlled within 0.25 - 0.33%.
- (3) The stiffness of FEM calculated curve is in good agreement with the measured curve at the early stage of loading. The calculated curve deviates from the measured curve during the middle and late stages. The calculated values are less than the measured ones. The error between the calculated and measured values is less than 15%.
- (4) According to the estimation, the structure is still in the elastic working range and has a high strength safety reserve under the circumstance of 8° seismic fortification intensity.

REFERENCES

- [1] Serrette R. L., José, Encalada, et al., 1997. Static racking behavior of plywood, OSB, gypsum, and fiber bond walls with metal framing. *Journal of Structural Engineering*, 123, 1079-1086.
- [2] Goggins J. M., Broderick B. M., Elghazouli A Y, et al., 2005. Experimental cyclic response of cold-formed hollow steel bracing members. *Engineering Structures*, 27, 977-989.
- [3] Landolfo R., Fiorino L., Corte G. D., 2006. Seismic behavior of sheathed cold-formed structures: numerical study. *Journal of Structural Engineering*, 132, 558-569.
- [4] Pourabdollah O., Farahbod F., Rofooei F. R., 2017. The seismic performance of K-braced cold-formed steel shear panels with improved connections. *Journal of Constructional Steel Research*, 135, 56-68.
- [5] Qian J. R., Song X. L., Feng B.C., et al., 2013. Experimental study and finite element analysis of seismic behavior of sprayed concrete sandwich shear walls. *Journal of Building Structures*, 34, 12-23. (in Chinese)
- [6] Hao Y. H., Mu L. H., WANG Y.Q., et al., 2013. Application study on CL building structure system in the construction of affordable housing. *Building Structure*, 43, 40-43. (in Chinese)
- [7] Zhou Q., 2006. The study of LIT composite concrete light-duty house system. Beijing University Of Civil Engineering And Architecture. (in Chinese)
- [8] Jia S, Cao W, Zhang Y., 2017. Damage index calibration of frame-supported concealed multi-ribbed wall panels with energy-efficient blocks. *Applied Sciences*, 7,453.
- [9] Mochizuki S., Kobayashi T., 1996. Experiment on slip strength of horizontal joint of precast concrete multi-story shear walls. *Journal of Structural & Construction Engineering*, 61, 63-73.
- [10] Chen J. S., Guo Z.X., 2012. Seismic Performance Study on Space Model of the New Precast Concrete Shear Wall Structure. *Construction Technology*, 41,87-89. (in Chinese)
- [11] Liu C.W., Cao W.L, Dong H.Y., et al., 2017. Test on seismic behavior of semi-assembled low-rise recycled concrete shear walls. *Journal of Harbin Institute of Technology*, 49,35-39. (in Chinese)
- [12] China Standards Publication, GB50011-2010, 2010. Code for seismic of design buildings; Standard Press of China: Beijing: China (in Chinese)
- [13] Cai J., Sun G., 2008. Constitutive relationship of concrete core confined by square steel tube. *Journal of South China University of Technology*, 36, 105-109.
- [14] Mander J. B., Priestley M. J. N., Park R, 1988 . Theoretical stress-strain model for confined concrete. *Journal of Structural Engineering*, 114,1804-1826.
- [15] Wang X., Li G., Shen Q.Z, 2005. Finite element analysis of the fly ash block walls strengthened by glass fiber reinforced plastics. *Industrial Construction*, 35, 96-98.